

Supporting Information for:

Theoretical investigation on electronic, optical, and charge transport properties of 7,8,15,16-tetraazaterrylene and its derivatives with electron-attracting substituents

Caibin Zhao^{a,b}, Wenliang Wang^{a,*}, Shiwei Yin^a, Yan Ma^a

^aKey Laboratory for Macromolecular Science of Shaanxi Province, School of Chemistry & Chemical Engineering, Shaanxi Normal University, Xi'an 710062, P. R. China

^bShaanxi University of Technology, School of Chemical & Environmental Sciences, Hanzhong 723001, P. R. China
E-mail: wlwang@snnu.edu.cn

Contents

Fig.S1 TAT single crystal viewed along the *b-c* plane (a), *a-b* plane (b), and *a-c* plane(c)

Fig.S2 Deviations between the computed HOMO and LUMO energies (E_H and E_L) as well as the HOMO- LUMO gaps (ΔE_{H-L}) and the measured values as a function of the basis set for TAT molecule

Fig.S3 Experimental (left) and optimized (right) geometries for TAT molecule

Fig.S4 Contribution of each vibration mode to the anionic relaxation energy for TAT and its derivates calculated at the B3LYP/6-311++G(d,p) level

Fig.S5 Simulated emission spectra for TAT and its derivates at the TD-DFT B3LYP/6-311G(d,p) level in chloroform solvent with the polarizable continuum model (PCM)

Fig.S6 Average squared displacement of 2000 times vs simulation time for TAT

Fig.S7 Dimer model of the dominated CT channel for TAT, 4F-TAT, 4Cl-TAT, and 4CN-TAT

Fig.S8 Schematic diagram of hole transfer integrals in the *a-b* plane of TAT single crystal (The molecules in the primate unit cell are represented by solid circles and open ellipses.)

Table S1 Calculated electronic properties for the planer (Optimized) and twisted (Experimental) TAT molecules based on the TPSSh/6-311G(d,p) and TPSSh/6-311++G(d,p) methods (in eV)

Table S2-S4 Optimized bond lengths of ground, cationic, anionic and the first-single excited states for 4F-TAT, 4Cl-TAT and 4CN-TAT at the B3LYP/6-311G(d,p) level (in Å)

Table S5 Absorption and emission properties for TAT and its derivates calculated at the TD-DFT B3LYP/6-311G(d,p) level in chloroform solvent with the PCM model along with attainable experimental values

Table S6-1 Calculated efficient parameters used in the Marcus-Levich-Jortner model

Table S6-2 Charge transfer rate constants calculated by the semiclassical Marcus-Hush and quantum-corrected Marcus-Levich-Jortner models (in s⁻¹)

Table S7 Calculated diffusion coefficients by the approximate relation and random-walk simulation technology for TAT (in cm²·s⁻¹)

* Corresponding author: wlwang Tel.: +86 29 8153 0815, Fax.: +86 29 8153 0727.

E-mail address: wlwang@snnu.edu.cn(W.L.Wang).

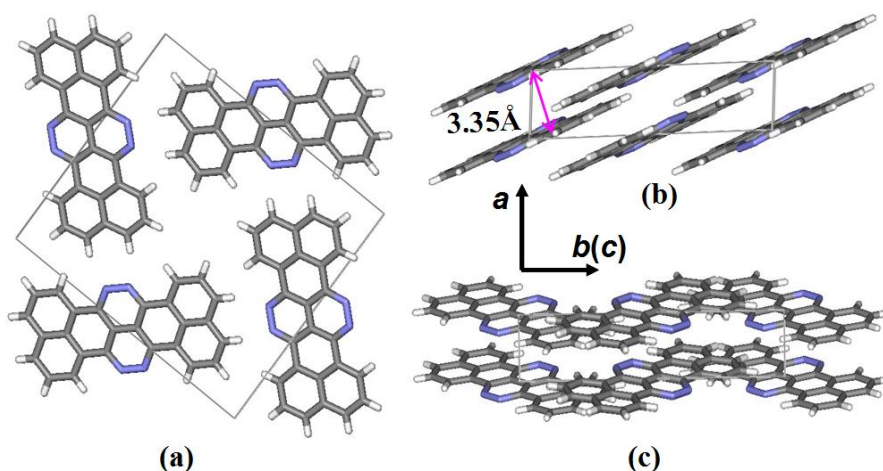


Fig.S1

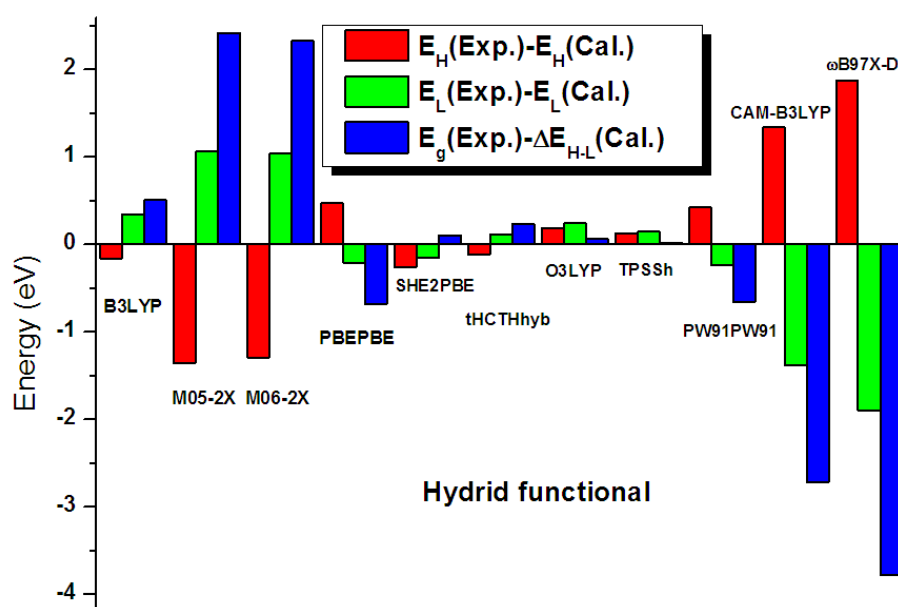


Fig.S2

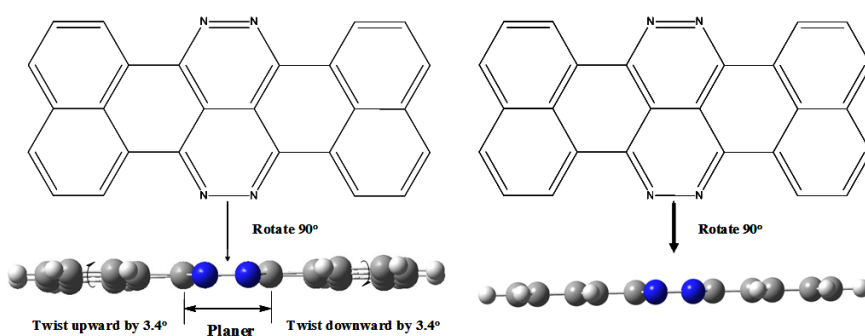


Fig.S3

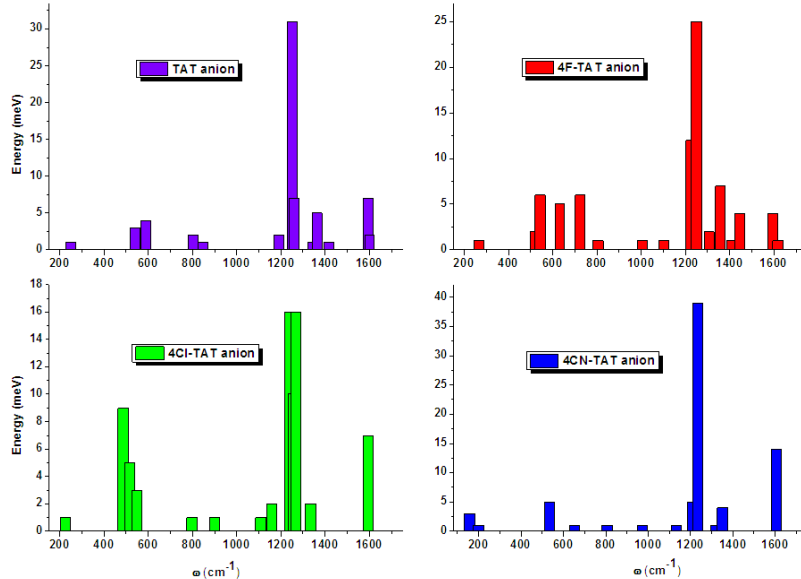


Fig.S4

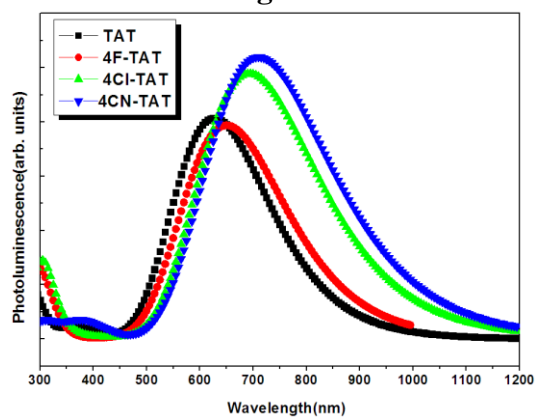


Fig.S5

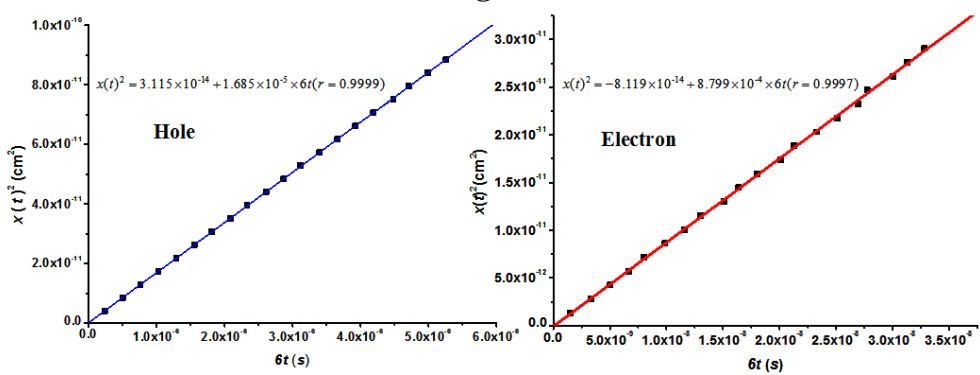


Fig.S6

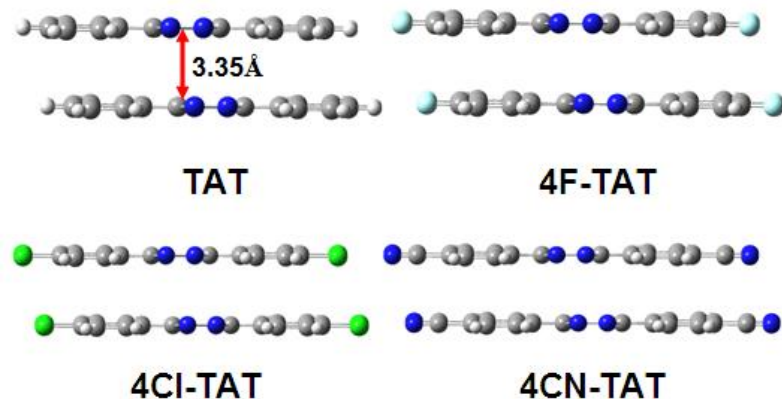


Fig.S7

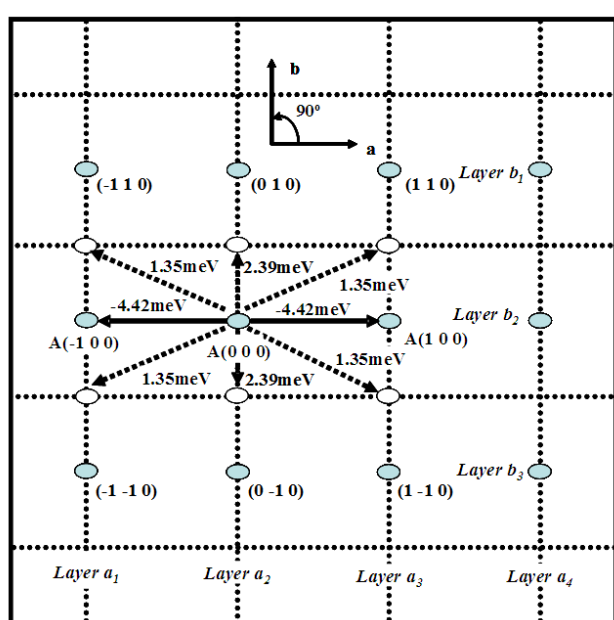


Fig.S8

Table S1

Basis set	Planer configuration		Twisted configuration	
	6-311G(d,p)	6-311++G(d,p)	6-311G(d,p)	6-311++G(d,p)
E _{HOMO}	-5.350	-5.405	-5.351	-5.410
E _{LUMO}	-3.355	-3.427	-3.271	-3.347
ΔE _{H-L}	-1.995	1.978	2.081	2.063

Table S2

	R ₁₋₂	R ₁₋₃	R ₂₋₄	R ₃₋₅	R ₄₋₆	R ₅₋₆	R ₄₋₇	R ₇₋₈	R ₈₋₉	R ₇₋₁₀	R ₁₀₋₁₁
Ground state	1.399	1.375	1.390	1.418	1.433	1.436	1.459	1.339	1.339	1.413	1.389
Cation	1.387	1.388	1.406	1.417	1.431	1.433	1.440	1.359	1.316	1.409	1.390
Δ(C-G)	-0.012	0.013	0.016	-0.001	-0.002	-0.003	-0.019	0.020	-0.023	-0.004	0.001
Anion	1.396	1.377	1.399	1.416	1.437	1.443	1.449	1.359	1.322	1.411	1.396

$\Delta(A-G)$	-0.003	0.002	0.009	-0.002	0.004	0.007	-0.010	0.020	-0.017	-0.002	0.007
Excited state	1.389	1.381	1.404	1.416	1.434	1.436	1.442	1.365	1.309	1.408	1.390
$\Delta(E-G)$	-0.010	0.006	0.014	-0.002	0.001	0.000	-0.017	0.026	-0.030	-0.005	0.001

Table S3

	R ₁₋₂	R ₁₋₃	R ₂₋₄	R ₃₋₅	R ₄₋₆	R ₅₋₆	R ₄₋₇	R ₇₋₈	R ₈₋₉	R ₇₋₁₀	R ₁₀₋₁₁
Ground state	1.391	1.379	1.382	1.434	1.436	1.454	1.463	1.335	1.338	1.409	1.385
Cation	1.379	1.394	1.398	1.435	1.433	1.451	1.442	1.356	1.313	1.404	1.387
$\Delta(C-G)$	-0.012	0.015	0.016	0.001	-0.003	-0.003	-0.021	0.021	-0.025	-0.005	0.002
Anion	1.385	1.384	1.393	1.430	1.439	1.463	1.450	1.356	1.318	1.405	1.392
$\Delta(A-G)$	-0.006	0.005	0.011	-0.004	0.003	0.009	-0.013	0.021	-0.020	-0.004	0.007
Excited state	1.381	1.390	1.399	1.432	1.437	1.456	1.443	1.365	1.310	1.403	1.388
$\Delta(E-G)$	-0.010	0.011	0.017	-0.002	0.001	0.002	-0.020	0.030	-0.028	-0.006	0.003

Table S4

	R ₁₋₂	R ₁₋₃	R ₂₋₄	R ₃₋₅	R ₄₋₆	R ₅₋₆	R ₄₋₇	R ₇₋₈	R ₈₋₉	R ₇₋₁₀	R ₁₀₋₁₁
Ground state	1.393	1.389	1.385	1.433	1.435	1.437	1.463	1.334	1.337	1.410	1.386
Cation	1.384	1.400	1.400	1.432	1.433	1.434	1.443	1.356	1.312	1.406	1.388
$\Delta(C-G)$	-0.009	0.011	0.015	-0.001	-0.002	-0.003	-0.02	0.022	-0.025	-0.004	0.002
Anion	1.382	1.400	1.398	1.432	1.438	1.444	1.447	1.356	1.315	1.407	1.393
$\Delta(A-G)$	-0.011	0.011	0.013	-0.001	0.003	0.007	-0.016	0.022	-0.022	-0.003	0.007
Excited state	1.385	1.396	1.395	1.433	1.437	1.439	1.438	1.359	1.359	1.412	1.396
$\Delta(E-G)$	-0.008	0.007	0.010	0.000	0.002	0.002	-0.025	0.025	0.022	0.002	0.010

Table S5

Compound	$\lambda_{\text{cal}}/\text{nm}$	f	$\lambda_{\text{exp}}/\text{nm}$	Main configuration
Absorption				
TAT	555.0	0.9695	537.4 ^a	HOMO→LUMO(100%)
	352.3	0.0554		HOMO-3→LUMO(92%)
	285.6	0.0441		HOMO→LUMO+5(59%) HOMO-8→LUMO(28%)
	280.5	0.0504		HOMO-3→LUMO+1(98%)
	276.8	0.0853		HOMO-8→LUMO(60%)
4F-TAT	560.8	0.9841		HOMO→LUMO(100%)
	298.5	0.1359		HOMO→LUMO+5(60%) HOMO-7→LUMO(21%)
	280.9	0.1713		HOMO-7→LUMO(71%)
	262.7	0.0638		HOMO-5→LUMO+1(93%)
4Cl-TAT	595.5	1.2187		HOMO→LUMO(100%)
	344.2	0.0212		HOMO-5→LUMO(85%)
	294.6	0.0111		HOMO-2→LUMO+2(96%)

	294.2	0.2681	HOMO→LUMO+5(+59%)
	279.4	0.0100	HOMO→LUMO+6(79%)
	266.3	0.0815	HOMO-5→LUMO+1(99%)
4CN-TAT	602.2	1.2911	HOMO→LUMO(100%)
	398.6	0.0121	HOMO→LUMO+2(95%)
	364.0	0.0737	HOMO-5→LUMO(91%)
	313.7	0.0211	HOMO-7→LUMO(85%)
	299.2	0.0110	HOMO-2→LUMO+1(85%)
	284.3	0.0801	HOMO→LUMO+5(37%) HOMO-6→LUMO+1(20%) HOMO-2→LUMO+3(16%) HOMO→LUMO+7(13%)
	627.1	1.0056	HOMO→LUMO(100%)
Emission TAT	393.0	0.0132	HOMO→LUMO+2(94%)
	296.9	0.0272	HOMO→LUMO+5(49%) HOMO-8→LUMO(45%)
	284.8	0.1808	HOMO-8→LUMO(46%) HOMO→LUMO+5(33%)
	275.1	0.0205	HOMO→LUMO+6(64%) HOMO-7→LUMO(30%)
	251.4	0.0121	HOMO-4→LUMO+2(93%)
	650.0	0.9720	HOMO→LUMO(100%)
	311.7	0.1149	HOMO→LUMO+5(54%) HOMO-7→LUMO(26%) HOMO-5→LUMO(15%)
4F-TAT	292.0	0.2173	HOMO-7→LUMO(66%) HOMO→LUMO+5(15%) HOMO-5→LUMO(10%)
	282.5	0.0276	HOMO-8→LUMO(63%) HOMO-2→LUMO+2(15%) HOMO→LUMO+6(20%)
	253.3	0.0268	HOMO-5→LUMO+1(97%)
	693.1	1.2079	HOMO→LUMO(100%)
	356.2	0.0159	HOMO-5→LUMO(86%)
	314.8	0.0212	HOMO-8→LUMO(77%) HOMO→LUMO+6(23%)
	304.5	0.2919	HOMO→LUMO+5(62%) HOMO-7→LUMO(18%) HOMO-5→LUMO(11%)
4Cl-TAT	299.0	0.0191	HOMO→LUMO+6(46%) HOMO-2→LUMO+1(38%) HOMO-8→LUMO(15%)
	292.8	0.0228	HOMO-2→LUMO+1(60%) HOMO→LUMO+6(29%)
	710.4	1.2829	HOMO→LUMO(100%)
	409.9	0.0152	HOMO→LUMO+2(93%)

380.5	0.0636	HOMO-5→LUMO(90%)
333.2	0.0280	HOMO-7→LUMO(86%)
324.9	0.0124	HOMO-8→LUMO(87%)
302.3	0.0119	HOMO-2→LUMO+1(63%) HOMO→LUMO+5(33%)

a Measured with UV-vis spectrum technology in chloroform solvent, from ref. 20.

Table S6-1

	TAT		4F-TAT		4Cl-TAT		4CN-TAT	
	hole	electron	hole	electron	hole	electron	hole	electron
λ_{class} (meV)	24	2	40	2	34	0	22	8
S_{eff}	1.944	1.026	1.508	1.354	1.345	1.282	0.973	1.031
ω_{eff} (cm ⁻¹)	846	1075	1232	974	1197	941	1224	1164

The calculation and selection of relevant parameters in Marcus-Levich-Jortner formulation:

$$k = \frac{2\pi}{\hbar} \frac{\left(V^{eff}\right)^2}{\sqrt{4\pi\lambda_{class}k_B T}} \sum_{n=0}^{\infty} \left[\exp(-S_{eff}) \frac{S_{eff}^n}{n!} \times \exp\left(-\frac{(\lambda_{class} + n\hbar\omega_{eff})^2}{4\lambda_{class}k_B T}\right) \right]$$

According to the MLJ equation, we need calculate the three important parameters, including λ_{class} , S_{eff} and ω_{eff} to obtain the CT rate constant k . Generally, the λ_{class} should include the outer reorganization energy and the contribution of some low-frequency mode vibrations. For the comparable purposes, we only consider the contribution of low-frequency vibrations (<250cm⁻¹) based on previous studies (Reference 31-32). The S_{eff} term is obtained directly the NM analysis by means of the DUSHIN program. All results are shown in Table S6-2.

Table S6-2

Pathway	Hole transfer		Electron transfer	
	Marcus-Hush model	MLJ model	Marcus-Hush model	MLJ model
1,6,9,14	0.0	0.0	4.057×10^8	3.459×10^8
2,5,10,13	4.228×10^7	3.453×10^7	7.152×10^{10}	6.098×10^{10}
3,4,11,12	1.825×10^{10}	2.282×10^{10}	1.491×10^{10}	1.946×10^{10}
7,15	0.0	0.0	2.116×10^8	1.804×10^8
8,16	1.024×10^{11}	8.366×10^{10}	3.153×10^{13}	2.688×10^{13}

Table S7

Hole transfer		Electron transfer	
approximate relation	random-walk simulation	approximate relation	random-walk simulation
2.290×10^{-5}	1.685×10^{-5}	6.240×10^{-3}	8.799×10^{-4}